J. Anat. (2005) **207**, pp783–796

Ultrastructural changes in the interhaemal membrane and junctional zone of the murine chorioallantoic placenta across gestation

P. M. Coan, A. C. Ferguson-Smith and G. J. Burton

Department of Anatomy, University of Cambridge, UK

Abstract

The mouse is an extremely useful experimental model for the study of human disease owing to the ease of genetic and physiological manipulation. A more detailed knowledge of murine placental development will, we hope, increase our understanding of the pathogenesis of placentally related complications of human pregnancy. The murine placenta consists of two main fetally derived compartments: the labyrinthine zone and the junctional zone. Exchange in the labyrinthine zone takes place across an interhaemal membrane comprising an outer layer of cytotrophoblast cells and two inner layers of syncytial trophoblast. The cytotrophoblast layer thins as gestation advances, and in addition becomes highly perforated after embryonic day (E)12.5. Furthermore, as gestation advances cytotrophoblast nuclear volume and DNA content increase, suggesting the formation of labyrinthine trophoblast giant cells. The syncytial layers become increasingly microvillous, enlarging the surface area for exchange. Separate basement membranes support the syncytium and the fetal capillary endothelium throughout gestation, although these appear to fuse where the capillaries are closely approximated to the trophoblast. The junctional zone consists of two principal trophoblast cell types, spongiotrophoblasts and invasive glycogen cells, yet the functions of each remain elusive. Spongiotrophoblasts vary in their appearance even when not fully differentiated, but a striking feature is the extensive endoplasmic reticulum of the more mature cells. Early glycogen cells are distinguished by the presence of electron-dense glycogen granules, and large amounts of surrounding extracellular matrix. Later the accumulations of glycogen granules occupy almost all the cytoplasm and there are few organelles. This is the first study to use both scanning and transmission electron microscopy in an ultrastructural description of murine placental development and is complementary to contemporary genetic investigations.

Key words development; electron microscopy; mouse; trophoblast.

Introduction

The recent realization that the intrauterine environment has a profound effect on predisposition to chronic illness in adult life (Barker, 2004) has led to a resurgence of interest in placental development and function. Because of the ease of genetic manipulation, the mouse is increasingly being used as an experimental model system to investigate placental development.

Correspondence
Dr P. M. Coan, Department of Anatomy, Downing Street, Cambridge CB2 3DY, UK. E: pmc40@cam.ac.uk

Accepted for publication *1 September 2005*

The structure of the murine placenta at the gross morphological and light microscopical levels has recently been reviewed (Georgiades et al. 2002; Malassiné et al. 2003), as have the molecular mechanisms underpinning cell lineage and differentiation (Rossant & Cross, 2001; Downs, 2002). Significant morphological differences exist between the human and the mouse placentas, but at the ultrastructural level comparisons are limited because little information is available for the mouse.

The definitive murine placenta contains cells of both fetal and maternal origin, and can be subdivided into three zones. Closest to the fetus is the labyrinthine zone (Lz), which consists of a complex interconnecting system of maternal blood spaces separated by trabecular cords

of fetal tissue containing fetal capillaries. Three layers of fetally derived trophoblast separate the fetal capillaries from the maternal blood, and hence the murine placenta is classified as haemotrichorial. The outer layer of trophoblast bathed directly by maternal blood (trophoblast Layer I) is cellular, the cytotrophoblast, whereas both the inner two layers (trophoblast Layers II and III) are multinucleated and syncytial in nature (Mossman, 1987). The labyrinthine zone is where nutrients, gas and waste are exchanged between mother and fetus, and as gestation progresses this compartment occupies the majority of the placental volume (Coan et al. 2004). However, the exact contribution each component of the trichorial membrane makes towards facilitation or impedance of exchange has yet to be revealed.

Separating the labyrinthine zone from the maternal uterine tissue is the junctional (Jz) or basal zone. This zone is a cellular compartment consisting of at least two distinct cell types after embryonic day (E)12.5: spongiotrophoblast (Spt) and glycogen cells (GCs). Both these cells express the junctional zone genetic marker *Tpbpa* and the spongiotrophoblast marker *Ascl2* (Cross, 2005). The function of this zone is yet to be fully understood (Georgiades et al. 2002), but it is essential for fetal survival as demonstrated by the *Ascl2–/–* mouse that lacks this zone and is lethal around E10.5 (Guillemot et al. 1994).

Bordering the junctional zone and the maternal decidua is a unicellular discontinuous layer of trophoblast giant cells (Pijnenborg et al. 1981). They are distinct from cells of the junctional zone in expressing the giant cell-specific marker *Hand1* (Hemberger & Cross, 2001). These large mononuclear, polyploid (Zybina & Zybina, 1996) trophoblasts produce a variety of hormones and chemokines (Malassiné et al. 2003), which may alter maternal physiology and immunology in order to accommodate the fetal allograft.

Detailed information of mouse placental development in terms of elucidating control of the differentiation of the various compartments by specific gene expression is rapidly accumulating (for reviews see Hemberger & Cross, 2001; Cross et al. 2003; Cross, 2005). Recently, there have also been advances in our understanding of uterine arterial remodelling, and of the diffusion properties of the placenta in normal and knockout mice (Adamson et al. 2002; Constancia et al. 2002; Sibley et al. 2004). Moreover, Adamson and colleagues have used both immunohistochemical techniques and vascular casting to describe the placental vasculature, and the relationship of maternal and fetal cells in placentas from E10.5 to E14.5 (Adamson et al. 2002).

Surprisingly, there are few publications on ultrastructural aspects of placental development in the mouse (but see Enders, 1965; Kirby & Bradbury, 1965; Björkman, 1970; Martinek, 1971). Of these, Martinek provided the most detailed account, but only of the maternal and fetal components at the deciduo–trophoblastic interface including the trophoblast giant cells. By contrast, Jollie (1964) and Davies & Glasser (1968) studied placental development in the rat. Jollie focused solely on the placental labyrinth and did not venture into description of the basal or junctional zone and the cell types therein. Davies and Glasser performed a comprehensive analysis of the placenta over gestation at the light microscope level with fine structural observations being made only at day 16 and without the use of glycogen-retaining post-fixation. To our knowledge, no studies have systematically explored changes with gestational age in the fine structure of the fetal placenta in the mouse, which includes the labyrinthine and junctional zones, using either transmission or scanning electron microscopy.

The present investigation was undertaken to determine ultrastructural changes in the interhaemal membrane during development and remodelling of the labyrinthine zone with gestational age that may underlie the increase in its diffusion properties (Sibley et al. 2004). Furthermore, a comprehensive description of cell phenotypes in the junctional zone has been carried out in order to elucidate the pattern of cell differentiation in this zone. At present no function can be attributed to the spongiotrophoblast cells but migration of glycogen cells into the decidua is thought to play a role in arterial remodelling (Georgiades et al. 2002).

Materials and methods

Animals

The C57BL/6J inbred mouse was chosen as it is a standard laboratory strain used in genomic analysis and experimental breeding strategies. All experiments were carried out in accordance with the UK Government Home Office licensing procedures. Matings were set up using virgin females (Harlan, UK) between 6 and

8 weeks old and housed under controlled laboratory conditions with a 12-h light/dark photoperiod. Animals were killed by cervical dislocation and placentas and fetuses dissected out and immediately placed in cold, sterile phosphate-buffered saline (PBS).

Transmission electron microscopy

Three mid-horn placentas from gestational ages E12.5, E14.5, E16.5, E18.5 and E19.5 were dissected from pregnant mice and immediately immersed in fixative. Tissue was fixed for 6 h with 4% glutaraldehyde in 0.1 M PIPES buffer, pH 7.2, washed with 0.1 M PIPES buffer and treated with 1% osmium ferricyanide. The post-fixed tissue was washed in 0.1 M PIPES buffer, and dehydrated. This was followed by washes in: propylene oxide; acetonitrile : Spurr's resin (1 : 1); Spurr's resin : acetonitrile (2 : 1), then overnight flat embedding in 100% Spurr's epoxy resin (Taab, UK). Spurr's resin was changed three times over 3 days, and the castings were thermally cured at 60 °C for 24 h. Sections 1 μm thick, close to the placental midline, were stained with Toluidine blue and used to identify regions of interest. Thin sections (50 nm) were stained with uranyl acetate and lead citrate, and viewed in a Philips CM100 at 80 kV.

Scanning electron microscopy

A pregnant mouse at E16.5 in gestation was killed by cervical dislocation and perfused with warm PBS containing heparin sulphate followed by 4% glutaraldehyde in 0.1 M PIPES buffer, pH 7.2. The post-fixed tissue was washed in 0.1 M PIPES buffer at 4 °C, and dehydrated. Tissue was then immersed in liquid nitrogen and fractured using a surgical scalpel. Fractured tissue was transferred to a critical point drier (Polaron E3000 CPD) using fresh, dry absolute alcohol and dried. Following drying, tissue was mounted onto SEM stubs and sputter coated with AuPd (Polaron E5000 Sputter Coater) to a thickness of 10 nm. Viewing was carried out on a Philips XL 30 FEG microscope at 5 kV.

Stereology

Resin sections, 1 μm thick, from four placentas at gestational ages E12.5, E14.5, E16.5 and E18.5, close to the placental midline were stained with Toluidine blue. The labyrinthine zone of each placenta was viewed using the ×100 objective lens. The CAST system including the Computer Assisted Stereological Toolbox (CAST) version 2.0 (Olympus, Denmark) program was used to select random fields of view within the labyrinthine zone for analysis. With a line grid, in random orientation, superimposed onto each field of view, unbiased point-sampled intercept lengths (PSI) were taken for the nuclei of all cytotrophoblast within fields of view. Where a line crossed a cytotrophoblast nucleus, the distance from one side of the nuclear membrane to the other along the line's length was measured. At least 200 PSI measurements were taken for placentas at each gestational age. The following equation was then used in order to estimate nuclear volume:

$$\bar{V}v = \frac{\pi}{3} \times \bar{l}_0^3$$

where $\bar{V}v$ is the mean volume-weighted nuclear volume and $\bar{l}_0^3$ is the mean of the cubed point-sampled intercept lengths (Gundersen & Jensen, 1985; Jensen & Gundersen, 1989).

Feulgen reaction

Paraffin sections of placenta at E14.5, E16.5 and E18.5 were dewaxed and rehydrated with the final step in distilled water. Slides were incubated in 5 N HCl for 1 h then rinsed for 7 min in distilled water. Feulgen stain (ScyTek Laboratories, UT, USA) was used to stain the cellular DNA for 1 h followed by rinses in distilled water and sulphurous acid rinse (Scytek Laboratories). Sections were dehydrated, cleared and mounted and digital images taken of systematic random fields of view within the labyrinthine zone of three placentas at the different gestational ages. Mean diameters of secondary giant cells and two populations of labyrinthine trophoblast cells were calculated using the CAST system. The Image J densitometry analysis program (http://rsb.info.nih.gov/ij/index.html) was then used to measure pixel density of whole nuclei from the digital images taken.

Statistical analysis

Statistical analysis was carried out with StatView version 5.0 (SAS Institute Inc.) using ANOVA and Fisher's protected least-significant difference *post-hoc* test.

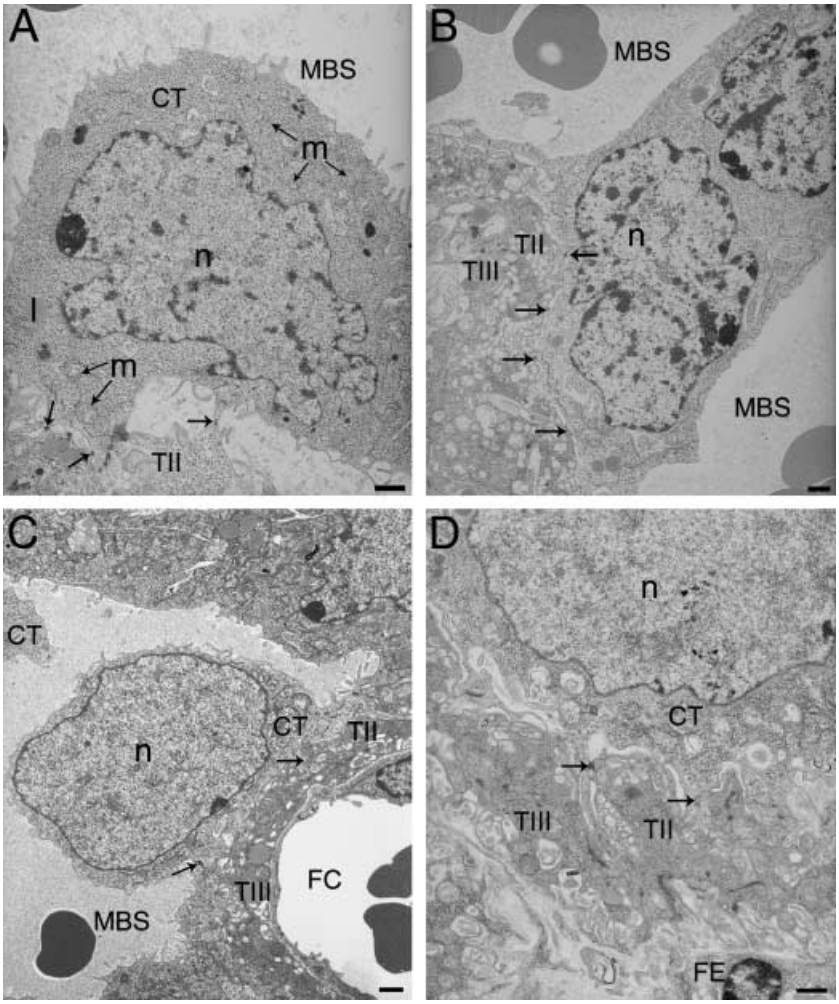

Fig. 1 Development of the cytotrophoblast with gestational age. (A) E12.5 cytotrophoblast (CT) attached to the underlying syncytial layer (TII) by desmosomes (indicated by arrows). (B) E14.5 binucleate cytotrophoblast spanning a maternal blood space (MBS). (C) E16.5 cytotrophoblast. (D) E19.5 cytotrophoblast intimately attached to the syncytial layer beneath (TII). FC, fetal capillary; FE, fetal endothelium; l, lipid droplet; m, mitochondrion; n, nucleus; T III, syncytial trophoblast Layer III. Arrows indicate desmosome adhesion complexes between cytotrophoblast and cytotrophoblast or syncytial trophoblast Layer II. Scale bar = 1 μm.

Observations

Labyrinthine zone

Trophoblast Layer I: cytotrophoblast layer

The cytotrophoblast cells form a continuous layer lining the maternal blood spaces in the early definitive placenta. Often, in a single focal plane there is one large nucleated cytotrophoblast cell profile that protrudes into each blood space (Fig. 1A,C), with its cytoplasm extending outwards across the underlying syncytium as a thin layer. The nuclei of cytotrophoblast cells at E12.5 are highly irregular in shape (Fig. 1A), and a prominent nucleolus is always present. There is some marginated electron-dense heterochromatin, and islands of heterochromatin are scattered within the otherwise electron-lucent euchromatin. Within the cytosol are small narrow cisternae of rough endoplasmic reticulum (RER), and numerous free ribosomes (15–25 nm) are dispersed throughout. Electron-lucent mitochondria are usually clustered around the nucleus (Fig. 1A). Vesicular structures of varying size and osmiophilia punctuate the cytoplasm, and include phagocytic vacuoles, exocytic/endocytic vesicles and lysosomes containing electron-dense material. Lipid droplets are commonplace in the nuclear and anuclear regions of the cytotrophoblast layer (Fig. 1A).

The cell membrane carries a series of short microvillous projections (Fig. 1A), which on the basal surface extend to make contact with neighbouring cytotrophoblast cells. No fusion takes place, however, and these cells remain in contact through adhesion complexes such as adherens or desmosome junctions. The layer is irregular in thickness, but no perforations are observed at this stage.

The structure remains broadly similar at E14.5 except that some cytotrophoblast cells have fused across a maternal blood space, creating an abundance of bridge forms (Figs 1B and 2A–F). By this stage the nuclei appear to occupy a larger volume in the cytotrophoblast

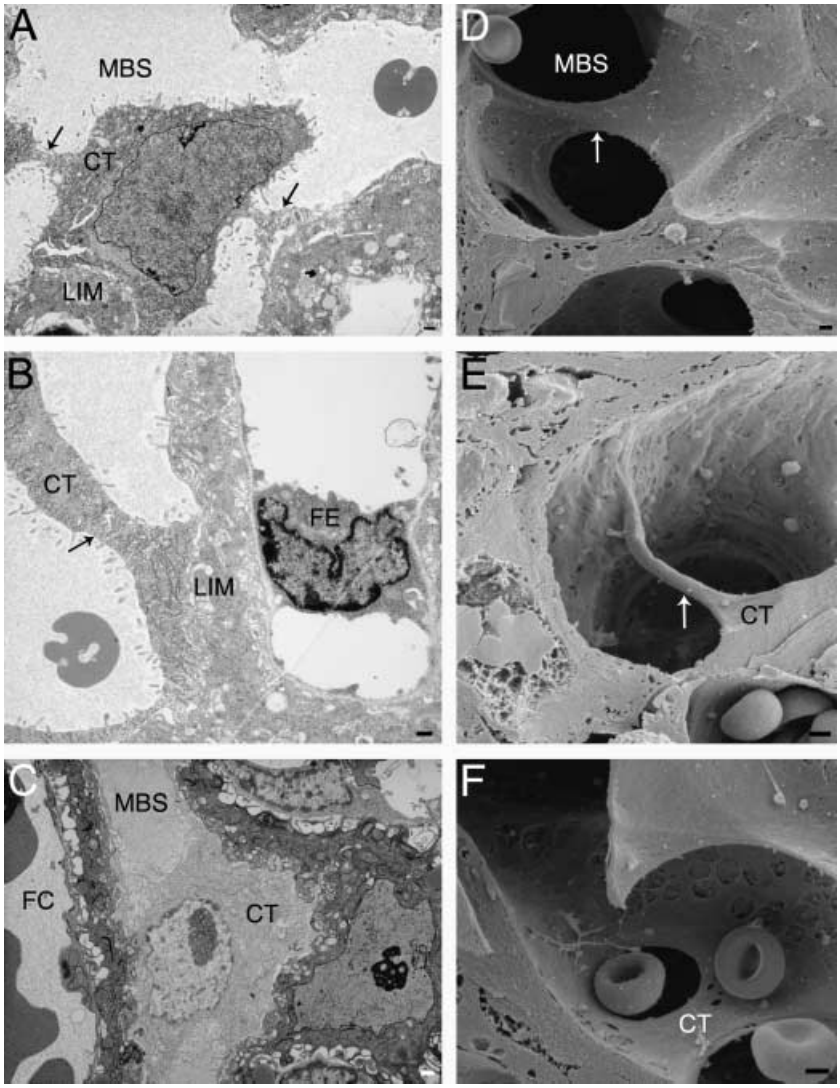

Fig. 2 Transmission and scanning electron micrographs of cytotrophoblastic bridges. (A) E14.5 cytotrophoblast (CT) with cytoplasmic bridges attached to several areas of labyrinthine zone interhaemal membrane (LIM) surrounding the maternal blood space (MBS). (B,C) E16.5 MBS adjacent to a fetal capillary (FC) with cytotrophoblast joining both sides of the LIM. (D–F) E16.5 labyrinthine zone with three-dimensional images of cytotrophoblast bridges. Arrows indicate cytotrophoblast bridges connecting separate sides of the lumens of blood spaces. Scale bar = 1 μm.

cells (Fig. 1B). They have more, and larger, patches of electron-dense heterochromatin as well as marginated heterochromatin. Perforations (0.5–2.0 μm in diameter) are present in the cytotrophoblast layer, and so maternal plasma has direct access to the underlying syncytial layer (Fig. 6A–F). Furthermore, apical protrusions from the syncytial layer beneath extend through the perforations, appearing to release secretions into the maternal blood (Fig. 6A,B).

At E16.5 trophoblast nuclei occupy the majority of the total cell volume (Fig. 1C). By this stage of development the nuclei are more regular in shape with a thin rim of dense heterochromatin surrounding otherwise electron-lucent euchromatin (Fig. 1C). There are few organelles present in the thin layer of cytoplasm surrounding the nucleus, and mitochondria occupy the more voluminous regions of the cytosol and the anuclear cytoplasmic regions lining the maternal blood space. Apical microvilli persist around the nucleated cell body, and are also extensive in the thinner anuclear regions of the cells (Figs 1C and 2A,B). Often there are distinct regions of the cytotrophoblast layer that are either highly microvillous or highly fenestrated (Fig. 6A–F).

Cytotrophoblast cells are attached to the underlying syncytium throughout gestation by desmosomes (Fig. 1D). At E12.5 there are relatively few junctional complexes between the two layers, and anchoring of the cytotrophoblast appears quite loose, with fluid-filled spaces extending between it and the syncytium (Fig. 1A). Later in gestation the nuclei of cytotrophoblast cells often project into the maternal blood space on a pedicle of cytoplasm, the basal surface of which widens and establishes a more intimate contact with the syncytium. By contrast, the peripheral anuclear regions

of the cytotrophoblast cells remain only infrequently attached to the underlying syncytial layer.

ANOVA demonstrated a significant increase in mean cytotrophoblast nuclear volume over gestation. *Post-hoc* testing revealed there is a doubling in the mean nuclear volume estimate between E14.5 and E16.5. However, there was no significant increase in volume between E12.5 and E14.5, or between E16.5 and E18.5 (Table 1).

The Feulgen reaction was used to quantify DNA content in the previously mentioned large labyrinthine cytotrophoblasts. These large cytotrophoblasts were categorized as being > 10 μm and were compared to the known polyploid secondary giant cells and diploid cytotrophoblasts, the nuclear diameter of which was < 10 μm. Using the Image J program, pixel density from Feulgen staining was determined to be proportional to DNA content. At each gestational age the large labyrinthine cytotrophoblasts had significantly greater DNA than the smaller diploid cytotrophoblasts (Table 2). However, this was not as great as the DNA content of the secondary giant cells, which had significantly more DNA than either the labyrinthine nuclei assessed (Table 2).

Trophoblast Layer II: syncytial trophoblast

The border between the cytotrophoblast layer and the first of the syncytial layers is undulating, and frequently processes from the cytotrophoblast cells appear to protrude into the syncytial layer, establishing a large surface area for exchange.

At E12.5 the syncytial layer appears quite disordered in appearance compared with later in gestation. There are few organelles within the electron-lucent cytosol (Fig. 3A), although free polyribosomes are disparately scattered throughout. In regions where the interhaemal membrane is thicker there are often accumulations of glycogen particles (30–90 nm). Small lipid droplets are infrequent, but there is an abundance of what appear to be micropinocytotic vesicles within the cytosol.

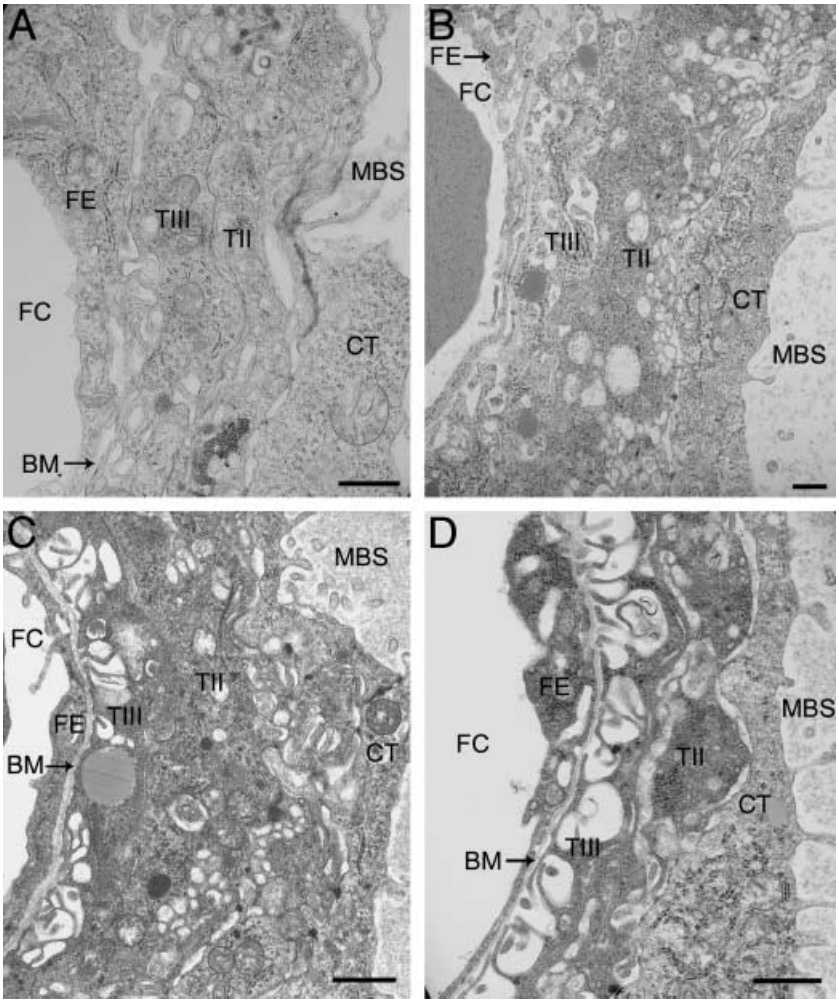

Fig. 3 Development of the labyrinthine interhaemal membrane with gestational age. (A) E12.5 interhaemal membrane showing maternal blood space (MBS) surrounded by cytotrophoblast (CT), directly apposed to the first syncytial trophoblast layer (TII), then the second syncytial trophoblast layer followed by basement membrane (BM), separating from the fetal endothelium (FE) that surrounds the fetal capillary (FC). (B) E14.5 interhaemal membrane. (C) E16.5 interhaemal membrane. (D) E18.5 interhaemal membrane. Scale bar = 1 μm.

Table 1 Mean (± SEM) volume-weighted cytotrophoblast nuclear volume over gestation measured using the point-sampled intercept method. Asterisks indicate homogeneous groups analysed by anova and Fisher's Protected Least Significant Difference

Gestational age (E)	12.5	14.5	16.5	18.5
Volume (μm^3)	393.1* ± 37	461.1* ± 39	808.5** ± 64	913.1** ± 136
		$P = 0.019$		

Table 2 Mean (± SEM) DNA content of large labyrinthine cytotrophoblast nuclei compared with small cytotrophoblast and secondary giant cell nuclei expressed as pixel density units. Asterisks indicate homogenous groups analysed by ANOVA and Fisher's Protected Least Significant Difference. CT, cytotrophoblast; TG, secondary giant cell

Trophoblast cell population	Gestational age (E)		
	14.5	16.5	18.5
Small CT nuclei (< 10 μm diameter)	107* ± 4	106* ± 3	135* ± 4
Large CT nuclei (> 10 μm diameter)	168** ± 4	182** ± 3	183** ± 4
TG nuclei (+ 40 μm diameter)	176*** ± 5	197*** ± 4	210*** ± 3
P	< 0.0001	< 0.0001	< 0.0001

The syncytial cytosol becomes more osmiophilic by E14.5 (Fig. 3B). There is an abundance of free electron-dense ribosomes that, in some cases, are bound to small cisternae of endoplasmic reticulum (ER). There are fewer, but larger, vesicular bodies than previously, sometimes containing an electron-lucent flocculent material. This layer varies greatly in thickness along its length and continues to have an erratic border adjacent to the cytotrophoblast layer.

Electron-density of the syncytial layer further increases by E16.5 (Fig. 3C). By this stage there are clusters of ribosomes, both attached to ER and free within the cytosol. Micropinocytotic profiles are rare, and there are few mitochondria, at least in regions of the syncytial layer directly between maternal blood space and fetal capillary. The degree of vacuolation is noticeably increased, particularly on the maternal face of this layer (Fig. 3B).

There is a progressive increase in vacuolation of the cytoplasm from E18.5 to term, and often flocculent electron-lucent matter is contained within these vacuoles (Fig. 3D). The convolutions on the maternal surface of Layer II are even more pronounced than at earlier stages and appear similar to an extensive microvillous system (Fig. 3D). The cytosol remains electron-dense and there are now fewer organelles present in those areas directly interposed between the two circulations. Generally, the layer is much thinner than previously, although the thickness is still highly variable along its length.

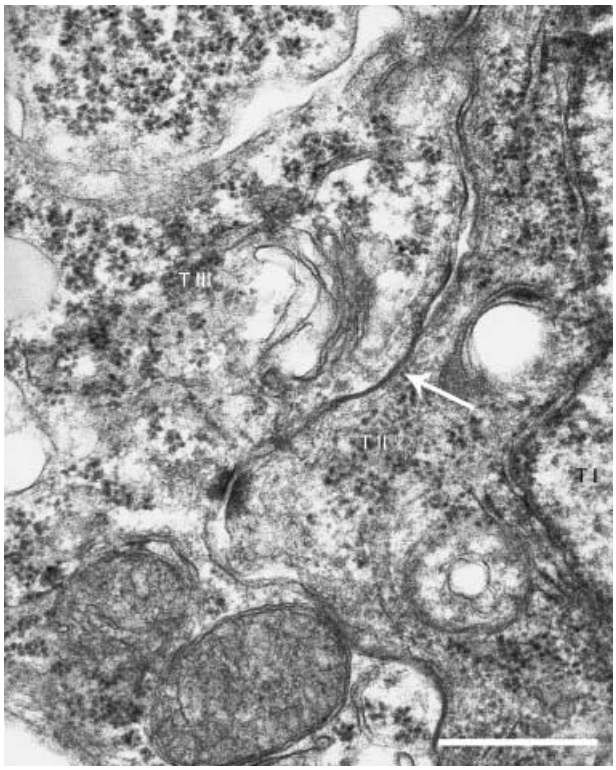

Fig. 4 Interhaemal membrane of an E16.5 mouse placenta illustrating where a gap junction, indicated by the arrow, is observed at the interface between syncytial trophoblast layers (T II & T III). T I, cytotrophoblast layer. Scale bar = 200 nm.

Trophoblast Layer III: syncytial trophoblast

The second syncytial layer of the mouse placenta is the thicker of the two, and again as gestation progresses the thickness becomes more variable from point to point. The interface between the two syncytial layers is slightly undulating, but there is no microvillous interdigitation, and the membranes are tightly attached by desmosomes. Gap junctions between the syncytial layers were observed frequently (Fig. 4).

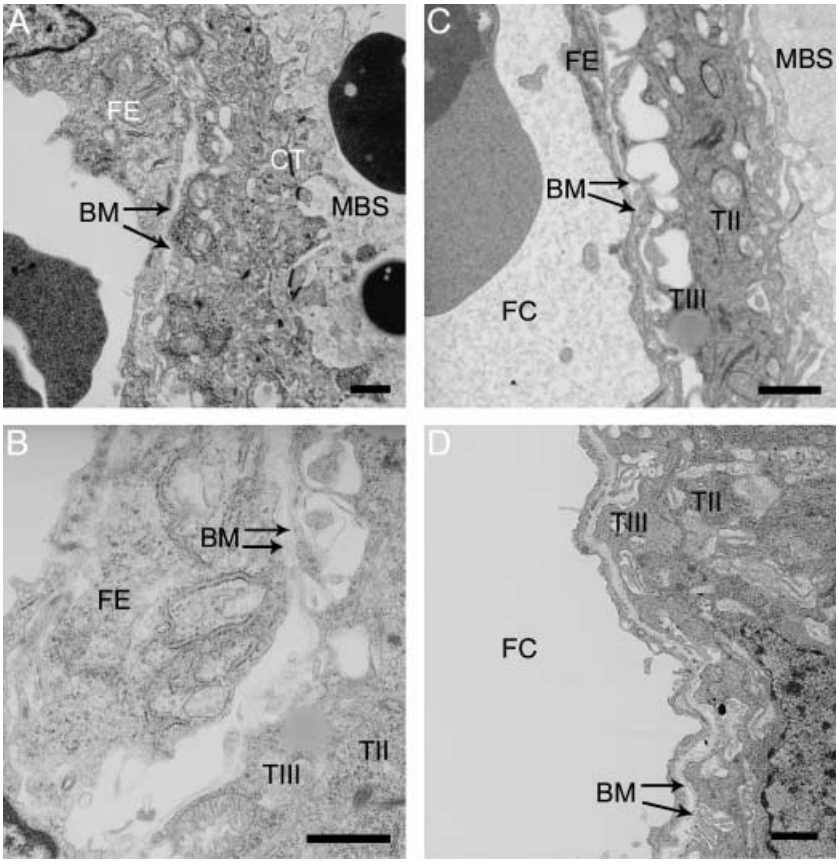

Fig. 5 Areas of the interhaemal membrane where two separate basement membranes (BM) can be clearly identified associated with the fetal endothelium (FE) or syncytial trophoblast (TIII) surrounding the fetal capillary (FC). (A) E12.5, (B) E14.5, (C) E16.5, (D) E19.5. CT, cytotrophoblast; MBS, maternal blood space; TII, syncytial trophoblast Layer II. Scale bar = 1 μm.

At E12.5 the cytosol of the second syncytial layer has a similar electron-lucency to that of Layer II, although it is generally less granular with fewer free ribosomes (Fig. 3A). Mitochondria are more prominent and frequently appear in thinner areas of the interhaemal membrane directly between maternal and fetal circulations. Lipid droplets are present, along with small regions of granular ER. The fetal surface of this layer has some degree of vacuolation though the microvillous plasma membrane is not evident by this stage.

By E14.5 the cytosol has become more osmiophilic and contains a few cisternae of RER. There are numerous lipid droplets and mitochondria, the contents of which are not easily resolved (Fig. 3B). On the fetal side of this layer the plasma membrane has become more convoluted although an abundance of microvilli is not present.

The E16.5 syncytial layer retains its electron-density. There are large, round, electron-dense mitochondria present, along with RER in thicker areas of the layer but otherwise fewer organelles when compared with Layer II (Fig. 3C). The extent and length of the basal microvillous protrusions is greater than at E14.5, further developing the surface area of the membrane on the fetal side. These projections often terminate in a bulb-like swelling, giving them the appearance of foot-processes (Fig. 3C).

From E18.5 to term the second syncytial layer becomes highly microvillous and few organelles are visible in areas of the layer that divide the two blood circulations. However, the density of the granular material within the cytosol has increased compared with earlier in gestation (Fig. 3D). There is a greater sophistication in plasma membrane structure, with an extensive microvillous system and large fluid-filled spaces between the trophoblast layer and the basement membrane.

Basement membranes

The trophoblast layer is supported on a well-developed basement membrane throughout gestation, and separate basement membranes also surround the fetal capillaries (Figs 5A–D and 6B). However, at each gestational time point, and for all placentas observed, areas were seen where the two appeared to have fused (Fig. 3A–D). Furthermore, the trophoblast basement membrane does not follow the convolutions of the microvillous

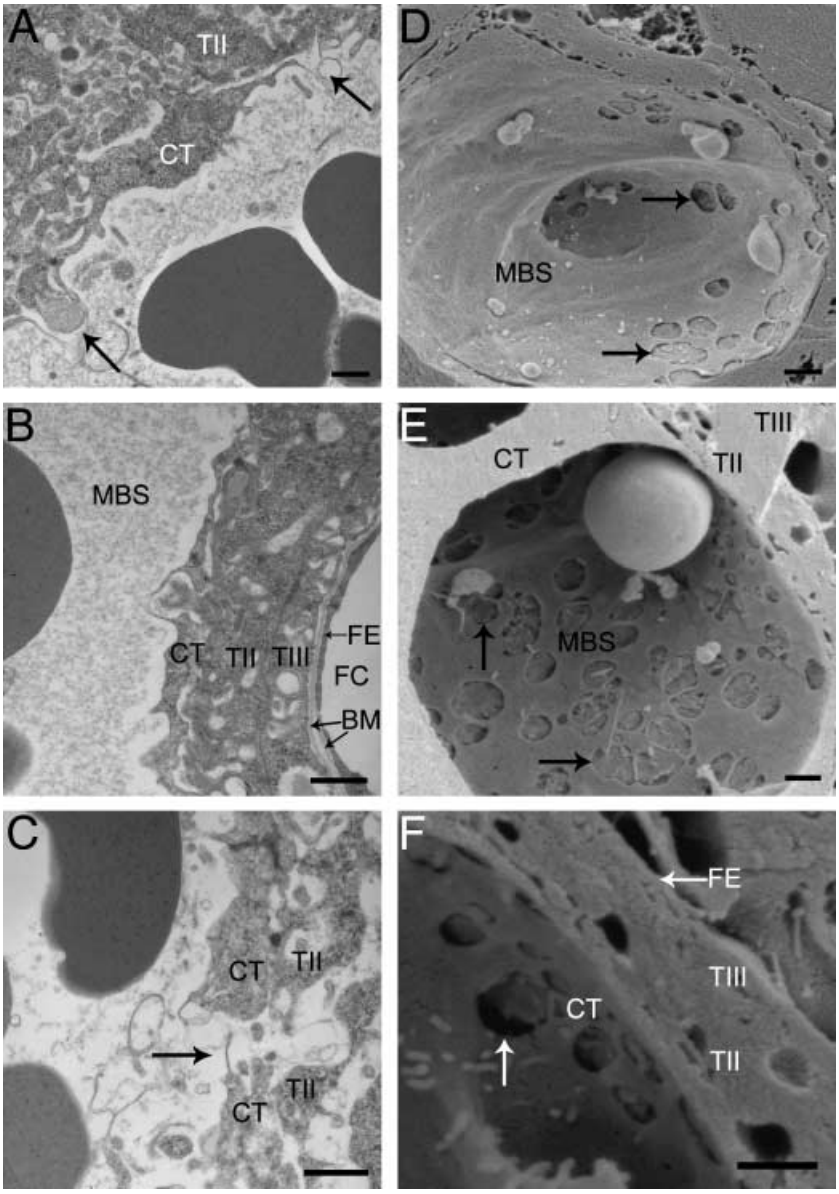

Fig. 6 Perforations in the cytotrophoblast layer. (A) E14.5 cytotrophoblast (CT) layer with two distinct perforations indicated by arrows, where the syncytial layer beneath appears to be secreting some electron-lucent material into the maternal blood. (B) E16.5 interhaemal membrane where the syncytial trophoblast layer (TII) has direct contact with maternal blood through the cytotrophoblast perforation. (C) E18.5 perforation directly over a channel running into the syncytial trophoblast layer beneath. (D–F) Scanning electron micrographs of E16.5 extensively fenestrated cytotrophoblast layer. BM, basement membrane; FC, fetal capillary; FE, fetal endothelium; MBS, maternal blood space; TIII, syncytial trophoblast layer. Scale bar = 1 μm.

system and instead remains more closely opposed to the endothelium. Towards term contact between the trophoblastic basement membrane and Layer III becomes increasingly tenuous as the basal surface of the latter becomes more extensively microvillous.

Fetal endothelium

The fetal endothelium remains unaltered in appearance throughout gestation. The nuclei are typical of endothelial cells, having an elongated shape, and there are large quantities of highly electron-dense marginated heterochromatin (Fig. 2B). The cytoplasm contains small mitochondria, numerous regions of ER, Golgi body and small cisternae of RER. There are occasional microvillous projections (Fig. 3C), and the cells are in close apposition with their basement membrane (Fig. 3A–D). The mouse endothelium does not regularly form fenestrations, but does become highly attenuated with increasing gestational age (Figs 2C,D, 3D and 5A–D).

Junctional zone

The junctional zone contains numerous venous sinuses lined by spongiotrophoblast cells that are filled with maternal blood draining back from the labyrinthine zone towards the decidua. After E14.5, glycogen cells can be seen to gather near these sinuses, but whether they

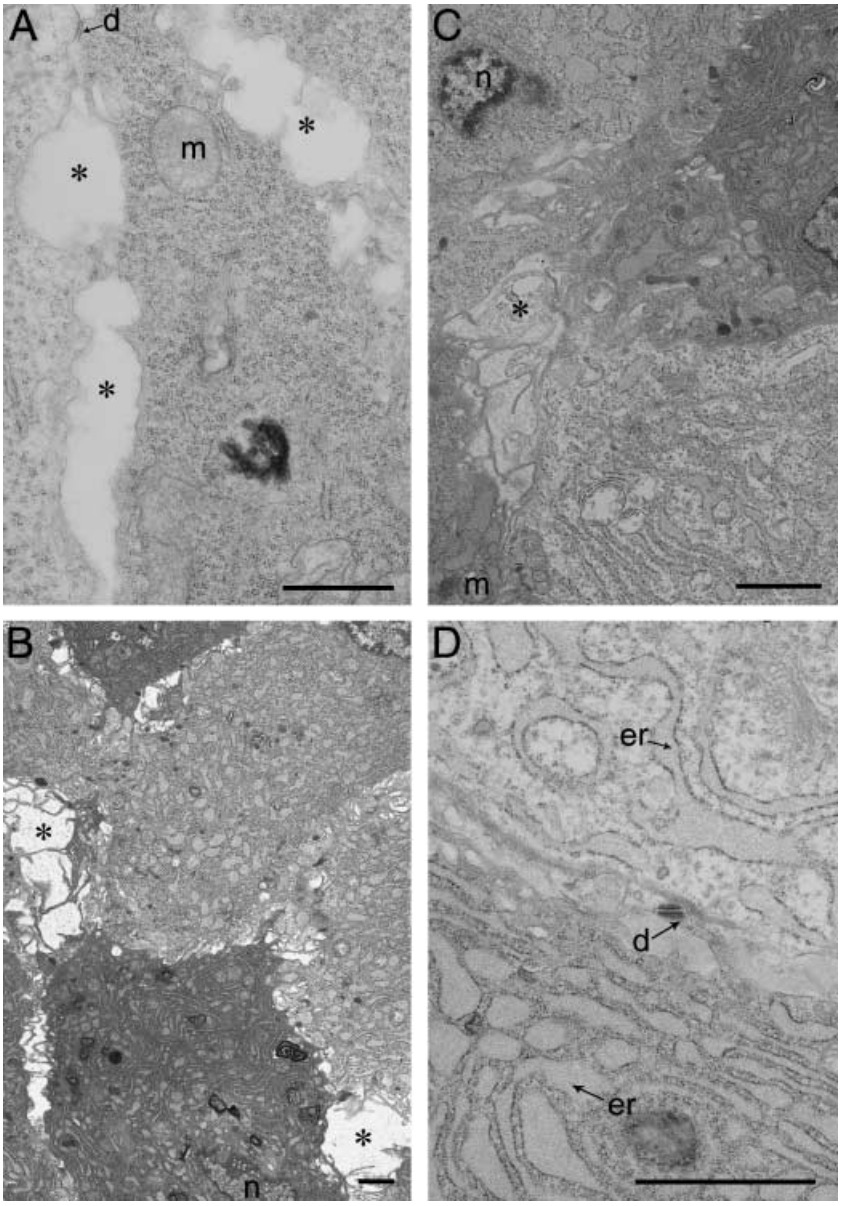

Fig. 7 Spongiotrophoblast development with gestational age. (A) E12.5, (B) E14.5, (C) E16.5, (D) E18.5. d, desmosome; er, endoplasmic reticulum; g, Golgi apparatus; m, mitochondrion; asterisks indicate fluid-filled spaces where spongiotrophoblast cytoplasmic projections are present. Scale bar = 1 μm.

have direct contact with maternal blood in the junctional zone remains to be investigated further (Fig. 8C,D).

Spongiotrophoblast

Within the Jz the Spt display a variety of different morphologies over the course of development.

At E12.5 the Jz is low in volume and contains predominantly Spt cells. By this stage, the migratory GCs are only just beginning to differentiate. The cytoplasm of Spt cells contains few organelles, suggesting these cells are undifferentiated (Fig. 7A). Nuclei differ in size, some appearing bilobed, and nuclear membranes may be highly infolded. Lipid droplets and electron-lucent mitochondria are abundant in the cytosol, as are groups of 3–8 free ribosomes. Cell–cell contact is generally quite intimate, but there are fluid-filled spaces, completely electron lucent, between some cells into which microvillous cytoplasmic processes project (Fig. 7A).

By E14.5 Spt cells vary in their electron density, and ER is a prominent feature. Spt cells contain predominantly RER with an extensive covering of ribosomes (Fig. 7B). Mitochondria are infrequent, but Golgi bodies and lipid droplets are present within the cytosol.

Later in gestation (E16.5) the Spt display a great variety of morphologies, but a generalized observation is dilatation of the RER cisternae. Some Spt have a completely electron-lucent cytoplasm, their ER cisternae

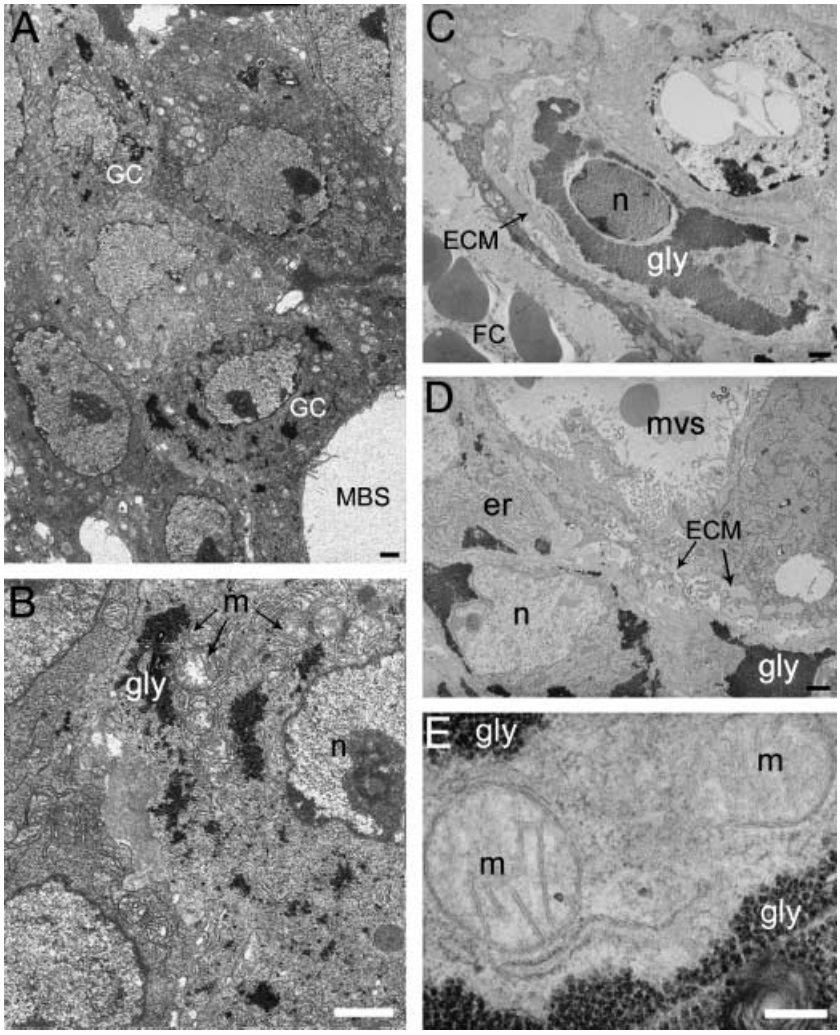

Fig. 8 Glycogen cell differentiation from E12.5 in gestation. (A) E12.5. (B) Close up of A. (C–E) E14.5. ECM, extracellular matrix; er, endoplasmic reticulum; FC, fetal capillary; gly, glycogen granules; m, mitochondrion; MBS, maternal blood space; mvs, maternal venous sinous in the junctional zone; n, nucleus. Scale bar = 1 μm (A–D), 200 nm (E).

containing electron-lucent flocculent material that appears identical to the extracellular matrix (ECM) surrounding GCs (Fig. 7C). The ER within the cells resembles a labyrinth of narrow electron-dense cisternae (Fig. 7D), and may form a lattice-like appearance creating boundaries around 'pools' of cytosol. In other Spt both the cytoplasm and the cisternae of the RER display greater electron density (Fig. 7B,D). Large Golgi structures are frequent (Fig. 7D).

Glycogen cells

At the light microscope level in the Jz of E12.5 placentas stained with Toluidine blue many clusters can be seen of darkly stained cells that are smaller than the majority of cells in the Jz. These clusters appear analogous to clusters of GCs at E14.5 and later.

From E12.5, GCs appear in the junctional zone. At this stage early GCs can be identified, already having small patches of glycogen granules accumulated within their cytoplasm and deposits of ECM surrounding the cell membranes (Fig. 8A). By E14.5 there are many more GCs that are organized into small clusters, or that are quite disparate throughout the Jz and maternal decidua (Fig. 8D). The ECM surrounding these cells remains, but now their cytoplasm contains large accumulations of glycogen granules (Fig. 8C,E). By E16.5 there are large clusters of GCs in the Jz and decidua and at the light microscope level the decidua appears to be heavily infiltrated by glycogen cells. These clusters decline in number and size by E18.5 and prior to term are less frequent in Jz.

GCs are surrounded by large deposits of ECM and rarely exhibit membrane adhesion complexes such as desmosomes (Fig. 8A–D). The nuclei of GCs are surrounded by what remains of the cytosol and the organelles. This region contains a high density of mitochondria, ER, vacuoles and sometimes lipid droplets.

However, organelles may also be found around the margin adjacent to the cell membrane. There is considerable variation in the quantities of marginated heterochromatin, and in the electron-density of the euchromatin and the heterochromatin clusters.

The typical morphology of GCs does not appear to alter once they have migrated into the maternal decidua.

Discussion

The chorioallantoic placenta of the mouse is a complex organ required to allow the fetus to survive and grow after mid-gestation, when the yolk sac becomes insufficient to cope with demands from the growing fetus. The two principal compartments, the labyrinthine and junctional zones, are distinguishable by E9.5, and undergo continual development and remodelling until term (Coan et al. 2004).

The interhaemal membrane is critical for materno-fetal exchange, and its surface area, composition and thickness are all important physical properties. The surface area of the maternal blood spaces increases from 3.6 cm^2 at E12.5 to 23.9 cm^2 at E18.5, and over the same period there is a reduction in arithmetic mean thickness of the interhaemal membrane from 10.6 μm to 4.8 μm (Coan et al. 2004). From the observations reported here it would appear that reductions in the thickness of the cytotrophoblast layer and of the capillary endothelium contribute most to this thinning. Thinning of the diffusion barrier is seen in all epithelia involved in gaseous exchange (Weibel, 1984), and on a theoretical basis this is one of the most significant factors influencing the rate of exchange (Mayhew, 1992). Conversely, Davies & Glasser (1968) suggested that there is an increase in thickness of the interhaemal membrane with gestation in the rat. This would seem improbable and impractical in terms of providing sufficient resources to the growing fetus, and requires validating by a quantitative study.

The small holes within the cytotrophoblast layer demonstrated so clearly here by scanning microscopy have previously been observed in the rat. Davies & Glasser (1968) described Layer I in the rat as an attenuated sheet, and went on to describe this phenomenon as 'cytotrophoblast fenestrations'. Because there is no membrane across these structures in the mouse or rat, which one would expect of a classical fenestration seen in capillaries in the kidney, we have used the term 'perforation' to avoid any confusion.

The perforations may play an important role in further thinning of the interhaemal barrier, as it is clear from the observations made here that maternal plasma has free access to Layer II of the trophoblast. This is consistent with previous reports that hydrophilic tracers introduced into the maternal circulation can later be observed between the cytotrophoblast and syncytial layers (Tillack, 1966; Wooding & Flint, 1994). In areas where there are no perforations, the cytotrophoblast cell membrane forms an abundance of microvillous structures that project into the maternal blood space. On the maternal side, cytotrophoblast and outer syncytial layers are actively involved in endo/exocytic processes important for maintenance of pregnancy. Thus, although the murine interhaemal membrane is classified as haemotrichorial morphologically, it may function physiologically more as a dichorial membrane, a notion proposed by Jollie for the rat (Jollie, 1964).

It is intriguing that the perforations are only observed from E14.5 onwards, when fetal demands are increasing. By allowing maternal plasma to circumvent Layer I, the presence of the perforations potentially avoids excessive oxygen extraction by the mitochondria present in the cytotrophoblast cells before the plasma reaches Layer II. The relative significance of this pathway to overall materno-fetal exchange will, however, depend in part on the rate of circulation of the plasma through the perforations, which needs to be determined experimentally. It is notable that in later gestation mitochondria were absent from those areas of Layers II and III interposed between the two circulations. This adaptation will again help to increase fetal oxygenation by reducing oxygen extraction by the placenta during transit of the gas across the interhaemal membrane. This arrangement is analogous to the subspecialization of the villous membrane of the human placenta into 'pneumatoid' and 'enteroid' regions (Kaufmann & Burton, 1994).

Further adaptations to facilitate materno-fetal exchange were seen on the deep surface of Layer III with increasing gestational age. The basal surface of Layer III expands its surface area vastly through formation of microvilli that, in accordance with Jollie's description of the rat placenta, end in foot-like processes that anchor the syncytium to the endothelial basement membrane (Jollie, 1964). This permits greater incorporation of transporter molecules, such as glucose transporter protein 3 (GLUT3) that have been immunolocalized to this region (P. M. Coan, unpublished observations). The fluid-

filled spaces between the projections may provide for the establishment of local concentration gradients that facilitate exchange.

Intercellular communication between syncytial layers in the mouse placenta is afforded in part by gap junctions. The rat placenta has also been described by Metz, who used freeze-fractured specimens to identify gap and tight junctions in cellular and syncytial parts for trophoblast Layers II and III (Metz, 1980).

Bounding the syncytial layers is the trophoblast basement membrane. It has previously been reported that only one basement membrane exists in the mouse placenta, common to both the trophoblast and the fetal capillaries (Georgiades et al. 2002). However, Kirby and Bradbury, who first described that the mouse placenta was in fact haemochorial, failed to note that their micrograph shows two basement membranes (fig. 2 in Kirby & Bradbury, 1965). Observations reported here confirm that a basement membrane exists for each of these structures in the mouse, but that when they are closely apposed fusion may occur. A similar situation has been reported for the human placenta (Enders, 1965). Fenestrations in the endothelial cells were not observed, although they have been reported previously in the mouse (Georgiades et al. 2002) and the rat placenta (Jollie, 1964).

An important new observation is that the perforations in the cytotrophoblast cells also appear to facilitate release of secretory products from Layer II into the maternal blood. The nature of these products is unclear, as the murine placenta does not produce chorionic gonadotropins or steroid hormones (Malassiné et al. 2003). Further work is required to identify these secretions.

It was observed in the rat placenta that there is an increase in the size of the cytotrophoblast cells in the labyrinthine zone over gestation, and that by E18.5 most, but not all, of the cytotrophoblast cells have partially 'transformed' into 'giant cells' (Davies & Glasser, 1968). A similar situation appears to exist in the mouse labyrinthine zone, as cytotrophoblast nuclear volume doubles across gestation, raising the possibility of endoreduplication. Soares et al. (1996) suggested that rat labyrinthine giant cells express placental lactogen II, and furthermore that the same situation is found in the mouse. However, we provide the first evidence that endoreduplication may have taken place in these large cytotrophoblasts in the mouse. Using the Feulgen reaction, in which staining colour intensity is directly proportional to DNA content (Chieco & Derenzini, 1999), we show a significant increase in DNA content between diploid cytotrophoblasts and the large cytotrophoblasts. Further research is required to investigate gene expression patterns in order to compare with known gene expression of the secondary giant cells bordering the maternal decidua. It was noted that as gestation advanced maternal blood spaces become subdivided by cytotrophoblast cells. These are clearly observed by using scanning electron microscopy, and sometimes take the form of thin sheets (Fig. 6D,F) or even just cell processes (Fig. 6E). On other occasions it appears that the cell bodies projecting into the blood space may come into contact or possibly even fuse, creating a binucleate cell (Fig. 1B). The physiological significance of this phenomenon is uncertain but it may serve to influence both the rate and the pattern of maternal blood flow through the labyrinthine zone.

In the junctional zone, by E12.5 the cell types appear undifferentiated, as evidenced by a lack of complex subcellular structure. There are at least two distinct populations of cells, however. The larger cells remain varied in size throughout gestation, although subpopulations appear to specialize in their functions as evidenced by distinct subcellular apparatus, or differences in electron density or lucency specific to certain cells. The physiological significance of this specialization is not known at present, but the large quantities of RER observed in this study suggest that they are actively synthesizing secretory proteins. The use of potassium ferricyanide during tissue preparation enabled the earliest stages of glycogen cell differentiation to be identified morphologically. Clusters of small cells containing patches of glycogen were observed, surrounded by thick deposits of ECM. No glycogen was present in any other cell in the junctional zone, strongly suggesting that these are early glycogen cells.

In a separate study using paraffin-embedded placentas from E12.5, early glycogen cells could be identified by Periodic Acid Schiff (PAS) positivity despite retaining an eosinophilic cytoplasm (data not shown). Whether in the junctional zone or decidua, glycogen cells retained PAS positivity, suggesting a continued retention of glycogen stores. No other cells or intercellular spaces in either the labyrinthine or the junctional zones were PAS positive, unlike the rat (Davies & Glasser, 1968).

The reason behind the large deposits of glycogen in glycogen cells is unknown, although one might speculate that it acts as an energy store for their migration. The

putative equivalent cell type in the human, the invasive extravillous trophoblast, is also observed to store quantities of glycogen early in its life span. Furthermore, secretion of large quantities of ECM is characteristic of invasive cell types, of which the glycogen cell is numerically the largest in the mouse placenta. The morphological identification of these early stages of differentiation will enable correlative studies to be performed with immunohistochemical markers, such as expression of $p57^{kip2}$, thus shedding further light on the molecular regulation of murine placental development.

Acknowledgements

We would like to thank Dr F. B. P. Wooding for his anti-GLUT3-stained sections, the Multiple Imaging Centre of the School of Biological Sciences and the Anatomy Visual Media Group. P.M.C. is funded by ASGBI and the Isaac Newton Trust of Trinity College, Cambridge.

References

Adamson SL, Lu Y, Whitely KJ, et al. (2002) Interactions between trophoblast cells and the maternal and fetal circulation in the mouse placenta. *Dev Biol* **250**, 358–373.

Barker DJ (2004) The developmental origins of chronic adult disease. *Acta Paediatr Suppl* **93**, 26–33.

Björkman N (1970) *An Atlas of Placental Fine Structure*. Oxford: Alder & Mowbray Ltd.

Chieco P, Derenzini M (1999) The Feulgen reaction 75 years on. *Histochem Cell Biol* **111**, 345–348.

Coan PM, Ferguson-Smith AC, Burton GJ (2004) Developmental dynamics of the definitive mouse placenta assessed by stereology. *Biol Reprod* **70**, 1806–1813.

Constancia M, Hemberger M, Hughes J, et al. (2002) Placental-specific IGF-II is a major modulator of placental and fetal growth. *Nature* **417**, 945–948.

Cross JC, Baczyk D, Dobric N, et al. (2003) Genes, development and evolution of the placenta. *Placenta* **24**, 123–130.

Cross JC (2005) How to make a placenta: mechanisms of trophoblast cell differentiation in mice – A review. *Placenta* **26**, S3–S9.

Davies J, Glasser SR (1968) Histological and fin structural observations on the placenta of the rat. *Acta Anat* **69**, 542–608.

Downs KM (2002) Early placental development ontogeny in the mouse. *Placenta* **23**, 116–131.

Enders AC (1965) A comparative study of the fine structure of the trophoblast in several hemochorial placentas. *Am J Anat* **116**, 29–68.

Georgiades P, Ferguson-Smith A, Burton GJ (2002) Comparative developmental anatomy of the murine and human placenta. *Placenta* **23**, 3–19.

Guillemot F, Nagy A, Auerbach A, Rossant J (1994) Rescue of a lethal mutation in Mash-2 reveals its essential role in extraembryonic development. *Nature* **371**, 333–336.

Gundersen HJG, Jensen EB (1985) Stereological estimate of volume weighted mean volume of arbitrary particles observed on random sections. *J Microsc* **138**, 127–142.

Hemberger M, Cross JC (2001) Genes governing placental development. *Trends Endocrin Metab* **12**, 162–168.

Jensen EB, Gundersen HJG (1989) Fundamental stereological formulae based on isotropically oriented probes through fixed points with applications to particle analysis. *J Microsc* **153**, 249–267.

Jollie WP (1964) Fine structural changes in placenta labyrinth of the rat with increasing gestational age. *J Ultrastruct Res* **10**, 27–47.

Kaufmann P, Burton GJ (1994) Anatomy and genesis of the placenta. In *The Physiology of Reproduction*, 2nd edn (eds Knobil E, Neill JD), pp. 441–483. New York: Raven Press Ltd.

Kirby DRS, Bradbury S (1965) The hemo-chorial mouse placenta. *Anat Rec* **152**, 279–282.

Malassiné A, Frendo JL, Evain-Brion D (2003) A comparison of placental development and endocrine functions between the human and mouse model. *Hum Reprod Update* **9**, 531–539.

Martinek JJ (1971) Ultrastructure of the deciduotrophoblastic interface of the mouse placenta. *Am J Obstet Gynecol* **109**, 424–431.

Mayhew TM (1992) The structural basis of oxygen diffusion in the human placenta. *Soc Exp Biol Sem Series* **51**, 79–101.

Metz J (1980) On the developing rat placenta. I. Differentiation and junctional alterations of labyrinthine layers II and III. *Anat Embryol* **159**, 289–305.

Mossman HW (1987) *Vertebrate Fetal Membranes*. London: Macmillan Press Ltd.

Pijnenborg R., Robertson WB, Brosens I, Dixon G (1981) Trophoblast invasion and the establishment of haemochorial placentation in man and laboratory animals. *Placenta* **2**, 71–92.

Rossant J, Cross J (2001) Placental development: lessons from mouse mutants. *Nat Rev Genet* **2**, 538–548.

Sibley CP, Coan PM, Ferguson-Smith AC, et al. (2004) Placental-specific Igf-2 regulates the diffusional exchange characteristics of the mouse placenta. *Proc Natl Acad Sci USA* **101**, 8204–8208.

Soares MJ, Chapman BM, Rasmussen G, Dai G, Kamei T, Orwig KE (1996) Differentiation of trophoblast endocrine cells. *Placenta* **17**, 277–289.

Tillack TW (1966) The transport of ferritin across the placenta of the rat. *Lab Invest* **15**, 896–909.

Weibel ER (1984) *The Pathway for Oxygen: Structure and Function in the Mammalian Respiratory System*. Cambridge, MA: Harvard University Press.

Wooding FBP, Flint APF (1994) Placentation. In *Marshall's Physiology of Reproduction*, 4th edn (Lamming GE, ed.), pp. 233–460 London: Chapman & Hall.

Zybina EV, Zybina TG (1996) Polytene chromosomes in mammalian cells. *Int Rev Cytol* **165**, 53–119.